42nd AIAA/ASME/SAE/ASEE Joint Propulsion Conference & Exhibit
9–12 July 2005, Sacramento, California

AIAA 2006-5233

Opposed Jet Burner Approach for Characterizing Flameholding Potentials of Hydrocarbon Scramjet Fuels

Gerald L. Pellett[*], Janet L. Convery[2], and Lloyd G. Wilson[3]

Abstract

Opposed Jet Burner (OJB) tools have been used extensively by the authors to measure Flame Strength (FS) extinction limits of laminar H_2/N_2–air and (recently) hydrocarbon (HC)–air Counterflow Diffusion Flames (CFDFs) at one atm. This paper details normalization of FSs of N_2-diluted H_2 and HC systems to account for effects of fuel composition, temperature, pressure, jet diameter, inflow Reynolds number, and inflow velocity profile (plug, contoured nozzle; and parabolic, straight tube). Normalized results exemplify a sensitive accurate means of validating, globally, reduced chemical kinetic models at ~ 1 atm and the relatively low temperatures approximating the loss of non-premixed "idealized" flameholding, e.g., in scramjet combustors.

Laminar FS is defined locally as maximum air input velocity, U_{air}, that sustains combustion of a counter-jet of g-fuel at extinction. It uniquely characterizes a fuel. And global axial strain rate at extinction (U_{air} normalized by nozzle or tube diameter, $D_{n \text{ or } t}$) can be compared directly with computed extinction limits, determined using either a 1-D Navier Stokes stream-function solution, using detailed transport and finite rate chemistry, or (better yet) a detailed 2-D Navier Stokes numerical simulation. The experimental results define an "idealized flameholding reactivity scale" that shows wide ranging (50 x) normalized FS's for various vaporized-liquid and gaseous HCs, including, in ascending order: JP-10, methane, JP-7, *n*-heptane, *n*-butane, propane, ethane, and ethylene. Results from H_2–air produce a unique and exceptionally strong flame that agree within ~1% of a recent 2-D numerically simulated FS for a 3 mm tube-OJB. Thus we suggest that experimental FS's and/or FS ratios, for various neat and blended HCs w/ and w/o additives, offer accurate global tests of chemical kinetic models at the Ts and Ps of extinction.

In conclusion, we argue the FS approach is more direct and fundamental, for assessing, e.g., idealized scramjet flameholding potentials, than measurements of laminar burning velocity or blowout in a Perfectly Stirred Reactor, because the latter characterize premixed combustion in the absence of aerodynamic strain. And FS *directly* measures a chemical kinetic characteristic of non-premixed combustion at typical flameholding temperatures. It mimics conditions where g-fuels are typically injected into a subsonic flameholding recirculation zone that captures air, where the effects of aerodynamic strain and associated multi-component diffusion become important.

---

[*] Senior Research Scientist, Hypersonic Air Breathing Propulsion Branch, Research and Technology Directorate. MS 168, NASA Langley Research Center, Hampton, VA 23681. Senior Member, AIAA g.l.pellett@larc.nasa.gov

[2] Graduate Student, National Institute of Aerospace, Hampton, VA; and Mechanical Engineering Department, VPI & SU, Blacksburg, VA; Member AIAA

[3] Technician, Lockheed Martin Space Operations, Hampton, VA

Introduction

For over 40 years, liquid hydrogen fuel has been used almost exclusively in studies aimed at realizing the potential of airbreathing Supersonic Combustion Ramjet (SCRAMJET) propulsion. Although liquid hydrogen is very difficult (and expensive) to use, it has remained the fuel of "choice," largely because of gaseous hydrogen's exceptional reactivity at near-atmospheric pressures, and to a lesser extent, its high specific impulse and unique capacity for active cooling. Liquid hydrocarbon (HC) fuels, on the other hand, have not been very useful for supersonic airbreathing applications because they are *far less reactive*, although they are obviously much easier to store and handle. Recently, endothermic catalytic cracking of HC fuels has also been investigated [1-2]. Difficult and competing objectives remain, however, to achieve ignition and robust combustion in relatively small subsonic cavity flameholders – so as to (a) generate rapid reaction with sufficient initial heat release, (b) avoid excessive internal drag and loss of net thrust, and (c) achieve needed "endothermic" heat soak in active cooling channels without the formation and deposition of significant carbon residues [2-8]. Thus catalytically cracked fuel vapor and entrained air must mix, diffuse and react long enough in a subsonic cavity to achieve ignition with robust "incipient flameholding," to supply radicals and adequate enthalpy to the overriding supersonic flow, with minimal loss of initial kinetic energy.

Opposed Jet Burner (OJB) tools have been used extensively by the authors to measure "Flame Strengths" at extinction of numerous laminar fuel–air Counterflow Diffusion Flames (CFDFs) at one atmosphere [9-20]. Early efforts focused on the velocity and thermal structure, and strain-induced extinction of 14 to 100% hydrogen–air CFDFs, summarized in [9]; the use of silane/hydrogen and silane/hydrocarbon mixtures for piloting very high speed combustion [10-11,16]; and the effects of vitiated air contaminants from test facilities on "incipient flameholding" in subsonic recirculating flows of an otherwise supersonic combustor [12-15,17,21,22]. These studies have shown that Flame Strength, FS, defined locally as the maximum air input velocity, U_{air}, which sustains combustion of a counterflowing jet of gaseous fuel just before extinction, represents a unique and important fuel-characterization parameter for "idealized" scramjet flameholding [21,22,9]. And, measurements of global axial strain rate, or Applied Stress Rate (ASR) at extinction (proportional to U_{air} normalized by either nozzle or tube diameter, $D_{n\ or\ t}$), can be compared directly with numerically simulated laminar extinction limits [18,19,9,23]. Such limits may be evaluated quite accurately using either a 1-D Navier Stokes stream-function approximation [20] with detailed transport and finite rate chemistry, or a fully detailed 2-D Navier Stokes numerical simulation [23].

This paper presents comprehensive data sets and analyses that represent an idealized Flame Strength (FS) approach to the assessment of so-called incipient flameholding limits in practical HC-air systems, near atmospheric pressure. It builds upon recent gaseous- and vaporized-HC FS results that were first presented [24] during the middle-phase of a MS study. Subsequently, that study included additional vaporized HC data, and details of normalizing vaporization and OJB extinction data to account for the effects of input temperature, pressure and jet diameter, and inflow Reynolds number and velocity profile (plug vs parabolic inflows) [25]. The present paper extends the [25] study by including additional HC–air and supporting H_2–air extinction data, and refined assessments of OJB strain rates from nozzle- and tube-OJBs to define better the effects of jet diameter, inflow velocity profile, Reynolds number, and fuel composition. The expanded sets of extinction data also help provide a more accurate and comprehensive means of globally validating reduced chemical kinetic models for HCs, at temperatures appropriate to strain-induced OJB extinctions *and* to the loss of non-premixed idealized, incipient flameholding in more complex scramjet combustors. The study concludes with a comprehensive normalization of the nozzle and tube OJB data that characterize steady (and dynamic [26-29]) strain-induced extinction of a very wide range of non-premixed fuel–air systems, near atmospheric pressure.

Experimental

Schematics of a typical nozzle-OJB (and Oscillatory-inflow nozzle-OJB) system, Fig 1a, and the most recent tube-OJB system, Fig. 1b, illustrate the use of convergent Pyrex nozzles, and long Pyrex, nickel or stainless steel tubes (50 to 100 diameters), of the same size and type. No guard flows were used (or seemed to be needed) at the typical flow rates employed for extinction of flat disk-shaped flames; horizontal configurations also favored formation of resultant ring-shaped flames and measurements of flame restoration. The ceramic fiberboard boxes each had Pyrex windows, and a porous sintered metal plate over the top. Nitrogen (or argon) entering through diffuser jets at the bottom of each box reduced extraneous combustion outside the central impingement region, and thus minimized adverse buoyancy and visibility effects. Fuel and air component flows were hand-controlled with micrometer valves, and measured by mass flow meters calibrated at 0 $^{\circ}$C and 1 atm.

To attain extinction (Blowoff) of a stabilized H_2/N_2–air disk flame, the H_2 flow was gradually increased -- or fixed at a target rate as N_2 fuel diluent was increased; simultaneously, the airflow was gradually increased, so the flame was always centered and free-floating (fully responsive to small changes in flow rates). Upon sudden Blowoff, a ring flame often stabilized. After mass flows of each component were recorded, gradual flow reductions caused slow closure of the ring flame, and eventually sudden disk Restoration. Extinction data were almost always obtained in duplicate, and were sometimes replicated up to 10 times. The same Blowoff limits of N_2–air could be reached by appropriate fixing of N_2 flows and decreasing H_2 flows. Similar procedures applied to obtaining extinction limits for gaseous HC/N_2–air and mixed H_2/HC–air and HC_1/HC_2–air systems, in that N_2 or HC diluent/reactant was increased in tandem with air to achieve extinction. Premixed and diluted vaporized-HC flows were simply varied in tandem with flows of air.

The reported cross-section-average jet velocities, U_{air} and U_{fuel}, were calculated from component mass flow rates and nozzle or tube exit diameters; these apply at 0 $^{\circ}$C and 1-atm conditions, unless attributed to 300 K, or higher. Corresponding Re_{air} were generally less than 1500, but considerably lower values were avoided, especially because CFDFs can become excessively thick when vertical, and also non-axisymmetric when horizontal, due to buoyancy. Radiation effects were considered negligible at the relatively high strain rates used.

The various tube-OJBs (1.8, 2.70, 2.91, 4.96, 5.0, 7.0, 7.5, and 10.0 mm) were mounted horizontally. The brass 5.3 mm nozzle was mounted horizontally, and the 2.7 mm, 5.1 mm and 7.2 mm Pyrex nozzle-OJBs were mounted vertically, with each upper element insulated to reduce convective heating of the fuel.

Both the 2.7 and 2.91 mm OJB's were spaced 7 mm apart to ensure a free-floating finite-thickness flame, free of significant flame attachment / anchoring effects. The larger tube- and nozzle-OJBs were generally spaced 1.5 to 2 exit diameters apart. Flow rates were generally high enough that buoyancy effects on flame extinction limits appeared negligible (and were, shown later) whenever data were recorded. Vaporized HC fuel mixtures flowed through electrically heated tubes, with thermocouple monitoring, before entering the OJB combustion chamber, so these fuels were heated up to 500-600 K to prevent condensation. Systematic checks of propane–air extinction limits using ambient temperature air, and unheated, rapidly-heated (5 min at 600 K), and long-term-heated propane (~ 2 hr at 600 K) showed very small difference in FS due to short term (1.5%) or long term (3%) heating of the fuel.

Errors in extinction limits stemmed from various sources. Because *absolute* strain rates at extinction were predicted (1-D) to vary linearly with input temperature, up to ~ 600 K [30,31], and experimental ASRs using a 2.7 mm tube-OJB were found to vary "nearly" linearly (e.g., with a

3

14% excess increase from 300 to 600 K [32]), direct measurements of mass flow rates effectively negated most effects of variable jet temperature on absolute jet velocity, via the ideal gas law. This led to significant reduction of data scatter with required input heating. Atmospheric pressure variations caused small variations of U_{air} extinction limits that were ignored (and averaged-out) during most of the hydrogen extinction studies, but more recently the HC and H_2 data were corrected [25] by applying a factor of $(1\text{-atm}/P)^3$. Calculated jet exit velocities at standard conditions varied inversely as the square of measured D, and thus ASRs varied as D^{-3}. Finally, un-reconciled small differences between data sets were due to unmeasured variations in atmospheric pressure (which sometimes averaged-out); differences in centering flames; daily jet realignment; sporadic mass flow meter drift, periodic re-calibrations, and small transient cooling/heating flow response effects in flow meters; and differences in the spatial distribution and flow rates of argon or nitrogen purge flows.

Because jet-edge velocity-mismatch and bath gas entrainment/diffusion effects were *incipient and evident* at high H_2 concentrations with the 2.7 mm nozzle-OJB [9], and also the flame thickness at extinction was ~ 1/3 D, the greatest uncertainty and non-ideality in our previous H_2– "clean air" extinction studies [9] is now believed to be associated with the 2.7 mm nozzle-OJB.

In summary, ideal, robust tube-OJBs (and the 7.2 mm nozzle-OJB) were the primary tools used for assessing strain-induced extinction limits of H_2/N_2–air and various HC/N_2–air CFDFs in the present study.

Results and Discussion

In this section we present several distinct sets of experimental results that help define key aspects of opposed jet combustion pertinent to the tools used, and the specific results obtained. Our results include the following: (**1**) A graphical summary of published Laser Doppler Anemometry (LDA) data will show detailed results for opposed cold flows from *finite size* contoured nozzles (D_n = 25 mm diameter). These will illustrate the effects of nozzle separation on axial and radial strain rates at fixed exit flow rates, and on various strain rate approximations suggested and adopted by two reseachers. One of these will exhibit a significant departure from measured strain rates when the nozzles are closely spaced (H/D_n << 1). (**2**) A series of OJB extinction and flame restoration results will be shown for N_2-diluted H_2 vs air CFDFs using tube-OJBs. These will illustrate significant effects of H_2 concentration and tube diameter, D_t, on the Flame Strength (FS = U_{air}) extinction limit, and the insensitivity of FS to tube spacing and tube orientation, e.g., two vertical and one horizontal. And these H_2–air FS results will be followed by an empirical fit of Applied Stress Rate (ASR = U_{air}/D_t) for all the FS data, for a wide range of tube diameters (1.8 - 10 mm) and H_2 concentrations (20 - 100%), for later comparisons with HC–air ASR extinction data. (**3**) A series of extinction results will be shown for N_2-diluted- and 100%-methane–air; these were derived from 7 mm tube-OJBs with vertical and horizontal orientations, and with fixed and variable tube-OJB spacing. (**4**) Two plots of ASRs will be shown for all the simple gaseous HC-air systems studied (five), and nearly all the OJB tube sizes used (7 sets, 2.7 – 10 mm). These will illustrate asymptotic approaches towards effectively constant ASR extinction limits for each fuel, as tube diameter increases relative to flame thickness, and as exit Reynolds number increases. (**5**) A series of HC-air extinction results will be shown, including pure and N_2-diluted methane and propane vs air from an early horizontal brass (5.3 mm) nozzle-OJB; and then N_2-diluted ethylene (20 - 80%) vs air from a "standard" vertical contoured-Pyrex nozzle-OJB (7.2 mm). The latter system has also been used extensively to characterize the dynamic weakening of the five gaseous HC-air systems [26-29], using steady plus oscillatory velocity inputs at frequencies from 8 to 200 Hz, where virtually all the weakening occurs, and then up to 1600 Hz. Note for all the above N_2-diluted H_2 and HC results, extinction limits will show

4

asymptotic approaches to nearly constant values as pure fuel is approached. This will indicate extinction limits unaffected by fuel diffusion rates to the airside flames, and hence extinctions limited by chemical kinetic rates. (**6**) The extinction results for gaseous HC fuels will be illustrated on a so-called "Idealized Flameholding Scale" consisting of ASRs from nozzle-OJBs plotted versus ASRs from tube-OJBs. This scaling technique will illustrate the relatively large effect of different axial velocity inflow profiles (plug vs parabolic) on ASRs for the various fuels, while maintaining simple proportionality to chemical kinetic reaction rates for the fuels. (**7**) The FSs of N_2-diluted n-heptane and JP-7 mixtures vs air will be shown, and will exhibit the same kinetically limited (asymptotic) behavior as with the gaseous HCs. Also, the n-heptane data will compare favorably with published extinction results (up to a 26 mole % limit) *when the published data, obtained at* relatively *small gaps, are appropriately corrected,* based on Rolon's LDA data. (**8**) A series of four figures will illustrate the strong effects on FSs of using methane, propane, and ethylene HCs to dilute H_2 (and to "scavenge" H-atoms), compared to the negligible effects of N_2 dilution on extinction limits at high H_2 concentrations (say, 80% – 100%). The same plots will also show the essentially negligible effects of initial H_2 dilution (addition to HCs) on FSs at low H_2 concentrations (say, 0 – 20%). Finally, (**9**) a comprehensive "Idealized Flameholding Scale" will be shown that includes all the results discussed above, extends a factor of 50 to pure H_2, and includes the effects of HC reactivity with H-atoms.

Measured and Estimated Strain Rates for Cold Opposed Flows

Fig. 2 shows a comparison of Rolon's LDA-measured strain rates (SRs) for varying separation of twin 25 mm diameter contoured nozzles, with fixed flows of air vs air and balanced axial jet momentum flux [33]. Both the measured radial SR, and – 1/2 the measured axial SR, are shown as a function of nozzle separation. In addition, Spalding's suggested approximation [34] for the radial SR, for very large uniform impinging flows, is U_{air}/D_n (also presently used as ASR for a convergent nozzle); it is only about 15% low of Rolon's measured values at $H/D \geq 1$. However, the $2U_{air}/H$ approximation developed by Williams [35], based on an assumed linear axial velocity gradient and balanced axial momentum fluxes for cold exit flows from large matrix type OJBs (typically 22 mm diameter), produces a SR that is *excessively large* under typical operating conditions ($H/D \sim 0.45$). Thus the reported SRs for the matrix burner are presently reduced by a factor of ~ 0.42 to match our short extrapolation of Rolon's measured radial SR (45 1/s). As pointed out by Rolon et. al [33], the $2U_{air}/H$ approximation only converges on the measured -1/2 axial and radial SRs well beyond $H/D > 1$, or preferably at ≥ 1.5. In our subsequent analysis of published n-heptane/N_2–air extinction data, derived from a 22 mm matrix burner [36], we applied the above correction factor of 0.42 to allow a SR data comparison (discussed later).

Nitrogen-diluted Hydrogen–Air Systems

Fig. 3 shows an early complete set of extinction (Blowoff) and flame restoration (Restore) data for N_2-diluted H_2 vs air CFDFs using a 2.7 mm tube-OJB. The physical / chemical effects of H_2 dilution by N_2 strongly impact both limits. The Blowoff data increase linearly at low H_2 concentrations, exhibit progressive non-linearity beyond 50% H_2, and achieve a well-defined horizontal asymptote for 80 to 100% H_2, which establishes a baseline for pure hydrogen (later, it will be shown that the presence of HCs, which typically react with H-atom, completely prevent the attainment of this asymptote). It has been shown earlier [15,17,9] that U_{air} is an especially relevant measure of CFDF extinction, compared to U_{fuel}, since the asymptotic U_{air} limit for $\geq 80\%$ H_2 reflects a *broad* regime of kinetically-limited H_2 combustion on the airside, unaffected by diffusion of fuel-jet N_2. Coincident with the U_{air} asymptote, a near doubling of U_{fuel} reflects the axial-input jet momentum flux balance for centering an ideal OJB flame, i.e., $\rho_{fuel} U_{fuel}^2 = \rho_{air} U_{air}^2$. This is typically well obeyed by the 2.7 mm tube-OJB at extinction. The hysteresis between Blowoff and Restore is obviously large, but its magnitude continues to grow proportionally with increased jet size. This is because U_{air} at Blowoff increases linearly with D,

and U_{air} at Restore is independent of D, for any given $X(H_2)$ and OJB type, since Restore corresponds to flame propagation just exceeding the outward radial flow of partially premixed fuel and air near the jet edge [9]; see also below.

Fig. 4 shows there is no effect of increasing tube separation (5 to 7.5 to 10 mm) on extinction and restoration limits of H_2/N_2–air CFDFs over a wide range of flowrates (~ 5 x), using a 5.0 mm horizontal tube-OJB. The enlarged hysteresis gap between Blowoff and Restore, compared to the 2.7 mm OJB results, is consistent with extinction SR being proportional to U_{air}/D_t, as discussed above.

Fig. 5 shows that OJB orientation had no effect on extinction and restoration limits of H_2/N_2–air CFDFs over a substantial range of flowrates, using both vertical and horizontal 7.0 mm Pyrex tube-OJBs at the "standard" OJB separation of $H/D_t = 2$. Thus, both Figs. 4 and 5 fully support the subsequent use of horizontal OJBs for HC-air extinction (and restoration) measurements.

Fig. 6 summarizes all the measured ASRs for extinction of H_2/N_2–air CFDFs, for a wide range of tube sizes and mostly horizontal orientations. Some upward-deviations of mid-range results from the two smallest OJBs (1.8 and 2.7 mm) typify the behavior (also seen later for HCs) of flames whose thickness is not small compared to tube diameter, at reduced Reynolds numbers. Note also the extinction-ASRs for tube-OJBs are systematically lower than for convergent nozzle-OJBs, due to the large effect of parabolic inflow profiles relative to plug flow profiles [9].

Gaseous Hydrocarbon–Air Systems

Fig. 7 shows the extinction of CH_4/N_2–air CFDFs using a 7.0 mm vertical-tube-OJB with fuel on top. The data exhibit a mild increase in FS (instead of a nearly flat asymptotic approach) as methane ranges 80% to 100%. This relatively minor deviation may reflect a tube orientation effect with a relatively weak flame, since data from a horizontal nozzle (shown later) exhibit a nearly flat asymptotic approach.

Fig. 8 shows that tube separation variations from 8 to 22 mm ($1 \leq H/D_t > 3$) had a negligible effect on FS for pure methane–air CFDFs, using a 7.0 mm horizontal tube-OJB. In the event that tube separation is reduced somewhat, to accommodate a weak flame that curves slightly upward due to buoyancy, the effect on FS is minimal. The average ASR (72.3 1/s) agrees closely with the averaged value for pure methane in Fig. 7 (72.2 1/s).

Fig. 9 summarizes the effect of OJB tube diameter on ASR at extinction for all the gaseous HCs studied thus far; and Fig. 10 shows the same ASR data plotted versus the product, $U_{air,300}$ * D_t, which effectively simulates the Reynolds number effect for similar gaseous systems. Clearly, the use of excessively small tubes produces ASRs that are artificially high compared to larger tubes, provided that extinction flows remain laminar. Tube diameters of 7 mm and higher resulted in ASRs that effectively reached horizontal asymptotic extinction limits for the five HCs. Thus the idealized Navier Stokes stream function solution for the 1-D Potential Flow boundary condition appears reasonable for the larger tube sizes and flow rates. Although a minor crossover of the propane–ethane data occurred near 5 mm diameter in each figure, relative ASRs among the HC–air systems are affected much less by tube diameter than are corresponding absolute values. Notably, the same relative effects have been found for nozzle-OJBs.

Fig. 11 shows respective FSs for N_2-diluted methane–air and propane–air systems derived from an early 5.3 mm brass horizontal-nozzle OJB. The nearly horizontal asymptotes for 80 to 100 mole % HC inputs for both fuels indicate (chemical) kinetically limited ASRs that are effectively independent of HC diffusion rate on the airside, similar to the behavior of H_2. Note these extinction ASRs for nozzles with plug inflows are substantially larger than shown earlier (Fig. 7) for tube-OJBs with parabolic inflows (quantified later).

6

Finally, Fig. 12 shows FSs for N_2-diluted ethylene–air systems, obtained using a "standard" 7.2 mm vertical Pyrex nozzle-OJB with 14 mm nozzle spacing. For this system, a horizontal asymptotic FS value for 100% C_2H_4 was estimated. The FS of ethylene was high enough that the fuel mass flowmeter just exceeded its operational limit. The same OJB system has also been used extensively to characterize dynamic flame weakening caused by sinusoidal velocity inputs of various (driven) amplitudes superimposed on steady inflows, with (mostly) in-phase frequencies ranging from 8 to 1600 Hz [26-29].

OJB-Extinction "Flameholding Scale" for Gaseous HCs

Fig. 13 shows the resultant OJB-extinction-limit, linear "Idealized Flameholding Scale" that was obtained for all the present gaseous HCs, using the 7.2 mm convergent Pyrex nozzle-OJB and the 7.5 mm straight tube-OJB (except for two sets of methane–air data from a 5.1 mm Pyrex nozzle and a 5.0 mm tube). Ethylene exhibits by far the highest Flame Strength (or ASR) of any HC tested. Note the highly linear relationship, with a slope of 2.51, represents a best estimate of the effective strain rate ratio for CFDF extinction based on tubes (parabolic inflow), compared with convergent nozzles (plug flow). The same ratio (2.5) also coincides nearly exactly with: (1) the respective axial *and* radial SR ratios (i.e., parabolic-inflow / plug-inflow) derived for *cold* flows, using a 2-D numerical simulation [23]; (2) the respective axial SR ratios derived for H_2–air CFDF *hot* flows, using the same 2-D numerical simulation [23]; and (3) a recently revised analysis [GLP manuscript in preparation] of earlier LDV measurements [19,9] of axial strain rates just upstream of H_2/N_2–air CFDFs using the respective 7.5 mm tubes and 7.2 mm nozzles.

Extinction of Pure and N_2-diluted Vaporized *n*-Heptane, JP-7 and JP-10 Fuels

Fig. 14 shows the results obtained for vaporized, and also nitrogen-diluted, n-heptane and JP-7 fuels [24,25]. The apparatus and general procedures used are shown and described in Fig. 1c. The respective ASRs increase substantially with increasing HC mole fraction up to about 75 mole %; thereafter, the ASRs attain respective horizontal asymptotic values, just as the gaseous HCs and hydrogen did. The asymptotes suggest, as before, chemical kinetic-limited ASRs, because each are unaffected by significant changes in nitrogen dilution. Although these neat fuels are of higher molecular weight and lower diffusivity than the gaseous HCs and H_2, and the axial-momentum-balanced flames (w/inputs of $\rho_{air} * U_{air}^2 = \rho_{fuel} * U_{fuel}^2$) should lie closer to the stagnation point, it still seems likely that pyrolysis and combustion-with-diffusion of lower molecular weight fuel species in the airside flame should continue being affected by nitrogen diffusion from the fuel side.

The solid points in Fig. 14, which agree quite closely with the present n-heptane data, represent substantially corrected experimental results originally published by Seiser et. al [36], who used a 22 mm diameter matrix-OJB with a gap of H = 10 mm. Thus the original (plotted) results were corrected to be comparable with the present ASR scale for a 7.5 mm tube-OJB. This correction has two parts. First, based on Rolon's measurements of axial and radial SRs as a function of nozzle separation distance [33], discussed earlier with Fig. 2, a correction factor of 0.42 was applied to the Ref. [36] matrix-OJB SR results of 500 1/s for 25 mole % *n*-heptane/N_2–air, and 400 1/s for 18 mole % *n*-heptane/N_2–air. The 0.42 factor estimates the *actual* radial (and -1/2 axial) SRs that existed at H/D_{burner} = 0.45, as a correction of the "standard" SR expression for a matrix-type burner, $2U_{air}/H$, that assumes a linear SR profile and an axial momentum balance for cold inflows. Next, SRs from the first stage of correction, which allow comparison with uniform-velocity (plug flow) ASRs from a convergent nozzle, were divided by a factor of 2.5. This equals both the experimentally- and numerically-derived factor (discussed above) that converts plug inflow ASRs for hydrocarbon–air systems to equivalent parabolic-inflow ASRs with the *same* radial strain rate in the flame core [23, and GLP et. al unpublished manuscript]. Note, because the equivalent H/D_{burner} = 0.45 separation of 11.25 mm in Fig. 2 is smaller than Rolon's smallest separation (15 mm), and Rolon's flows were cold, the first part of the correction is slightly uncertain.

Figs. 15 and 16 show some of the original batch-process liquid-vaporization data used to produce *n*-heptane/N_2 mixtures at elevated temperature and pressure, in preparation for subsequent multiple determinations (typically 8 to 10 acceptable measurements) after heat-up and stabilization of the nitrogen-purged combustion chamber [24,25].

Reactivity of Hydrogen plus HC mixtures

Figs. 17-19 show extinction data for HC-diluted H_2 vs air, where methane, propane, and ethylene are used, respectively, to dilute pure hydrogen. All three sets of results show a *dramatic decrease* in FS as HC is added initially; and this also leads to a rapid convergence of Blowoff and Restore limits [16]. These initial decreases can be compared directly with the Fig. 3 results for N_2 dilution, which exhibit an unchanging asymptotic FS from 80-100 mole % H_2. The physical explanation for these dramatic decreases in FS is these simple HCs are very effective in scavenging H-atoms that normally form, diffuse rapidly on the airside, and dominate flame reactivity. Thus the reduction in H-atom (and OH) greatly reduces FS [16,9]. Also, at the HC-rich (left) end, as H_2 is initially added to each HC, the data show *very little increase* in FS as H_2 increases 0 to 20 %. In a similar vein, H-atoms resulting from incremental H_2 addition are so effectively scavenged by HCs that FS is totally dominated by the HC. Both of these results have significant implications with respect to any contemplated use of HC plus H_2 mixed fuels, whether at the H_2-rich end (used to retard combustion), or at the HC-rich end (e.g. barbatage). And finally, ignition of mixed HC plus 10% H_2 fuels has been found to exhibit similar behavior [3].

Comprehensive "Idealized Flameholding Scale" for HCs, H_2 and Mixtures

Fig. 20 shows a major extension of the Fig. 13 linear "Idealized Flameholding Scale" obtained for simple gaseous HCs. As before, the 7.2 mm Pyrex nozzle- and the 7.5 mm straight tube-OJBs characterize each of the simple HCs. However, the plot also contains additional 100% H_2 data, HC-plus-H_2 data extracted from the high-FS regions of Figs. 17 and 19, and also three sets of recent pure- and nitrogen-diluted vaporized-liquid FS data. The latter data for 100% JP-10–air, and both pure and nitrogen-diluted JP-7 and *n*-heptane vs air, were obtained as part of a recent MS thesis by JLC [25], and this followed a paper presented near the mid-point of the study [24].

In Fig. 20, 100% H_2, which produces a unique and exceptionally strong flame, bounds the upper end of the flameholding scale. Both data points (averaged from previous 2.7 mm Pyrex nozzle- and 2.7 mm tube-OJB data; and obtained from a recent 2.91 mm tube-OJB) agree within about 1% of Hwang's recent 2-D numerically simulated FSs for hydrogen-air extinction, for a 3 mm tube-OJB configuration with appropriate guard flows and disk-shaped boundary conditions [23]. For all the data points marked with a pound sign (#), measurements made with respective 7.5 mm and 2.7 mm tube-OJBs were plotted on a least-squares fit of all the gaseous HC data, *plus* the early data for pure H_2 from 2.7 mm nozzle- and 2.7 mm tube-OJBs. Although the linear slope increased from 2.51 to 2.73 due to addition of the pure H_2 data, the former slope (2.51) is now considered most appropriate for HC CFDFs. This is largely due to a now recognized downstream shift in the average HC flame location, on the airside, relative to that for hydrogen [GLP manuscript in preparation].

Based on the above FS characterizations, and the very wide range of reactivity exhibited on the Idealized Flameholding Scale of Fig. 20, we conclude that the experimental ASR's, and/or ratios of ASR's for various neat and blended hydrocarbons with and without additives, represent relative global chemical kinetic limits. As such, the ASRs can provide absolute and relative tests of the validity of reduced chemical kinetic models, when applied at the appropriate pressures and peak temperatures of extinction.

Comparison of Flame Strengths with Laminar Burning Velocities

Fig. 21 compares ASRs for all the gaseous-HC extinction limits, from the 7.5 mm tube-OJB, with recently surveyed / published unstrained laminar burning velocity, $S_{L,0}$, measurements

[37,38] at an equivalence ratio of unity (phi = 1). And, Fig. 22 extends the ASR results of Fig. 21 all the way to 100% H_2. Clearly, the ASRs reflect considerably more sensitivity to changes in fuel molecular size and reactivity than $S_{L,0}$ does. In Fig. 21, a linear fit of the ASR vs $S_{L,0}$ data leads to a slope of 3.64, which seems inappropriately small for the (four lowest) saturated HCs. And in Fig. 22, a power-law fit of the gaseous-HC + H_2 data seemed to represent the only reasonable fit of the data. In this case a power law exponent of 1.87 fit the overall data quite well. This further demonstrates a strong apparent "dependence" of ASR on $S_{L,0}$. Thus, in conclusion, we find that burning velocity changes only weakly against strain-sensitive FS variations, and this leads us to recommend that laminar burning velocity is a relatively insensitive and unsatisfactory measure of fuel reactivity changes, for use in assessing "idealized" flameholding at atmospheric pressure.

Summary and Conclusions

This paper details the normalization of FSs of N_2-diluted H_2 and HC systems to account for effects of fuel composition, temperature, pressure, jet diameter, inflow Reynolds number, and inflow velocity profile (plug, contoured nozzle; parabolic, straight tube). Normalized results exemplify a sensitive accurate means of validating, globally, reduced chemical kinetic models at ~ 1 atm and temperatures approximating the loss of non-premixed "idealized" flameholding, e.g., in scramjet combustors.

Laminar FS is defined locally as maximum air input velocity, U_{air}, that sustains combustion of a counter-jet of g-fuel at extinction. It uniquely characterizes a fuel. And global axial strain rate at extinction (U_{air} normalized by nozzle or tube diameter, $D_{n\ or\ t}$) can be compared directly with computed extinction limits, determined using either a 1-D Navier Stokes stream-function solution, using detailed transport and finite rate chemistry, or a detailed 2-D Navier Stokes numerical simulation. The experimental results define an "idealized flameholding reactivity scale" that shows wide ranging (50 x) normalized FS's for various vaporized-liquid and gaseous HCs, including, in ascending order: JP-10, methane, JP-7, *n*-heptane, *n*-butane, propane, ethane, and ethylene. Results from H_2–air produce a unique and exceptionally strong flame that now agree within about 1% of a recent 2-D numerically simulated FS for a 3 mm tube-OJB. Thus we suggest that experimental FS's and/or FS ratios, for various neat and blended HCs w/ and w/o additives, offer accurate global tests of chemical kinetic models at the temperatures and pressures of extinction.

We conclude the FS approach is more direct and fundamental, for assessing, e.g., idealized scramjet flameholding potentials, than measurements of laminar burning velocity or blowout in a Perfectly Stirred Reactor, because they characterize premixed combustion in the absence of aerodynamic strain. And FS *directly* measures a chemical kinetic characteristic of non-premixed combustion at typical flameholding temperatures. It mimics conditions where gaseous fuels are typically injected into a subsonic flameholding recirculation zone that captures air, where the effects of aerodynamic strain and associated multi-component diffusion are important.

Based on the above results, we advocate that a remotely operated OJB system be developed to achieve real-time (e.g., 1 minute) characterizations of the idealized flameholding potential (FS) of high-T, high-pressure, multi-component, vaporized-hydrocarbon fuels being used for scramjet testing. Results should also be compared with other relevant sources of vaporized HCs, e.g., fuels processed by simple bench top vaporizer / catalytic cracking systems, or fuels captured by "freezing" the composition of a cracked vaporized (superfluid) HC from a heater / vaporizer / catalytic-cracking system. Thus we propose that measurements of FS could be, and should be, a key routine HC fuel characterization parameter for any scramjet combustor test. Similar logic may be applied to the development of any surrogate HC fuel mixture, such that its measured FS mimics that of a typical uncracked- and also cracked fuel, and its FS can be numerically simulated for a known composition, using available chemical kinetics and a detailed OJB code.

References

1. Maurice, L.Q., Corporan, E., Minus, D., Mantz, R., Edwards, T., Wohlwend, K. Harrison, W.E., Striebich, R.C., Sidhu, S. Graham, J., Hitch, B., Wickham, D, and Karpuk, M., "Smart Fuels: "Controlled Chemically Reacting Fuels," AIAA Paper AIAA 99-4916, July, 1999, 11 pp.

2. Wickham, D.T., Alptekin, G.O., Engel, J.R., and Karpuk, M.E., "Additives to Reduce Coking in Endothermic Heat Exchangers," AIAA Paper AIAA 99-2215, July, 1999, 9 pp.

3. Colket, M.B., III, and Spadaccini, L.J., "Scramjet Fuels Autoignition Study," J. Propulsion and Power, **17**, No. 2, 2001, Mar.-Apr. 2001pp. 315-323.

4. Gruber, M. Dunbar, J., and Jackson, K., "Newly Developed Direct-Connect High-Enthalpy Supersonic Combustion Research Facility," J. Propulsion and Power, **17**, No. 6, Nov.-Dec. 2001, pp. 1296-1304.

5. Mathur, T., Gruber, M., Jackson, K., Donbar, J., Donaldson, W., Jackson, T., and Billig. F., "Supersonic Combustion Experiments with a Cavity-Based Fuel Injector," J. Propulsion and Power, **17**, No. 6, Nov.-Dec. 2001, pp. 1305-1312.

6. Rasmussen, C.C., Driscoll, J.F., Hsu, Kuang-Yu, Donbar, J.M., Gruber, M.R., and Carer, C.D., "Stability Limits of Cavity-Stabilized flames in Supersonic Flow," Proceedings of the Combustion Institute **30** (2005), 2825-2833.

7. Cooke, J.A., Bellucci, M., Smooke, M.d., Gomez, A., Violi, A., Faravelli, T. and Ranzi, E., "Computational and Experimental Study of JP-8, a Surrogate, and its Components in Counterflow Diffusion Flames," Proceedings of the Combustion Institute **30** (2005), 439-446.

8. Maurice, L.Q, Edwards, T., Cuoco, F. Bruno, C, and Hendrick, P., CHAPTER 2: Fuels, in *Technologies for Propelled Hypersonic Flight*, RTO-TR-AVT-007, Volume 2 – Subgroup 2: Scram Propulsion, ISBNs 978-92-837-0041-4 / 978-92-837-0041-8, Jan. 2006, pp. 2-1 through 2-35.

9. Pellett, G.L., Isaac, K.M., Humphreys, W.M., Jr., Gartrell, L.R., Roberts, W.L., Dancey, C.L., and Northam, G.B., "Velocity and Thermal Structure, and Strain-Induced Extinction of 14 to 100% Hydrogen-Air Counterflow Diffusion Flames," *Combust. Flame* **112**, No. 4, 1998, pp. 575-592.

10. Pellett, G.L., Northam, G.B., Guerra, R., and Wilson, L.G., "Opposed Jet Burner Studies of Silane-Methane, Silane-Hydrogen, and Hydrogen Diffusion Flames with Air," CPIA Publication 457, Vol. 1, Oct. 1986, pp. 391-404.

11. Pellett, G.L., Northam, G.B., Wilson, L.G., "Counterflow Diffusion Flames of Hydrogen, and Hydrogen Plus Methane, Ethylene, Propane, and Silane, vs. Air: Strain Rates at Extinction," AIAA Paper 91-0370, Jan. 1991, 17 pp.

12. Guerra, Rosemary, Pellett, G.L., Wilson, L.G., Northam, G.B., "Opposed Jet Burner Studies of Hydrogen Combustion with Pure and N_2, NO Contaminated Air," AIAA Paper 87-0090, Jan. 1987, 11 pp.

13. Guerra, Rosemary, Pellett, G.L., Wilson, L.G., Northam, G.B., "Opposed Jet Burner Studies of Effects of CO, CO_2 and N_2 Air Contaminants on Hydrogen-Air Diffusion Flames," AIAA Paper 87-1960, July 1987, 14 pp.

14. Pellett, G.L., Jentzen, M.E., Wilson, L.G., and Northam, G.B., "Effects of Water-Contaminated Air on Blowoff Limits of Opposed Jet Hydrogen-Air Diffusion Flames," AIAA Paper 88-3295, July 1988, 10 pp.

15. Pellett, G.L., Wilson, L.G., Northam, G.B., Guerra, Rosemary, "Effects of H_2O, CO_2, and N_2 Air Contaminants on Critical Airside Strain Rates for Extinction of Hydrogen–Air Counterflow Diffusion Flames," CPIA Publication 529, Vol. II, (Oct., 1989), pp. 23-42. Pasadena, CA, Oct., 1989.

16. Pellett, G.L., Northam, G.B., Wilson, L.G., "Counterflow Diffusion Flames of Hydrogen, and Hydrogen Plus Methane, Ethylene, Propane, and Silane, vs. Air: Strain Rates at Extinction," AIAA Paper 91-0370, Jan., 1991, 17 pp.

17. Pellett, G.L., Northam, G.B., Wilson, L.G., "Strain-Induced Extinction of Hydrogen–Air Counterflow Diffusion Flames: Effects of Steam, CO_2, N_2, and O_2 Additives to Air," AIAA Paper 92-0877, Jan., 1992, 15 pp. (Also a manuscript in preparation on these and recent 2-D numerical results.)

18. Pellett, G. L., Roberts, W. L., Wilson, L. G., Humphreys, W. M., Jr., Bartram, S. M., Weinstein, L. M., and Isaac, K. M., "Structure of Hydrogen–Air Counterflow Diffusion Flames Obtained by Focusing Schlieren, Shadowgraph, PIV, Thermometry, and Computation," AIAA Paper 94-2300, June 1994, 23 pp.

19. Pellett, G. L., Wilson, L. G., Humphreys, W. M.,Jr., Bartram, S. M., Gartrell, L. R., and Isaac, K. M., Roberts, W. L., IV, and Northam, G. B., "Velocity Fields of Axisymmetric Hydrogen-Air Counterflow Diffusion Flames from LDV, PIV, and Numerical Computation," AIAA paper 95-3112, July 1995, 23 pp.

20. Isaac, K. M., Ho, Y. H., Zhao, J., Pellett, G. L., and Northam, G. B., "Global Characteristics and Structure of Hydrogen-Air Counterflow Diffusion Flames: A One-Dimensional Model," AIAA Paper 94-0680, Jan.,1994. Also, Zhao, J., Isaac, K. M., and Pellett, G. L., *J. Propul. Power* **12**, No. 3: 534-542 (1996).

21. Pellett, G.L., Bruno, C., and Chinitz, W., "Review of Air Vitiation Effects on Scramjet Ignition and Flameholding Combustion Processes," AIAA Paper 2002-3880, July 2002, 37 pp.

22. Pellett, G.L., Bruno, C, and Chinitz, W., CHAPTER 4: Air Vitiation Effects on Scramjet Combustion Tests, in *Technologies for Propelled Hypersonic Flight*, RTO-TR-AVT-007, Volume 2 – Subgroup 4: Scram Propulsion, ISBNs 978-92-837-0041-4 / 978-92-837-0041-8, Jan. 2006, pp 4-1 through 4-21.

23. Hwang, Kyu C., "Two Dimensional Numerical Simulation of Highly-Srained Hydrogen–Air Opposed Jet Laminar Diffusion Flames," Ph. D. Dissertation, Old Dominion University, Norfolk, VA, May 2003.

24. Convery, J.L., Pellett, G.L., O' Brien, W.F., and Wilson, L.G., "An Experimental Study of *n*-Heptane and JP-7 Extinction Limits in an Opposed Jet Burner," AIAA Paper 2005-3766, July 2005, 8 pp.

25. Convery, J.L., "An Experimental Investigation of JP-7 and *n*-Heptane Extinction Limits in an Opposed Jet Burner," MS Thesis in Mechanical Engineering, Virginia Polytechnic Institute and State University, Blacksburg, VA, October 27, 2005, 52 pp.

26. Pellett, G.L., Reid, Beth, McNamara, Clare, Johnson, Rachel, Kabaria, Amy, Panigrahi, Babita, and Wilson, L.G., "Acoustic Weakening of Methane-, Ethylene-, and Hydrogen-Air Counterflow Diffusion Flames, and Implications for Scramjet Flameholding." AIAA Paper 2003-4634, July 2003, 21 pp.

27. Pellett, G., Reid, B., McNamara, C., Johnson, R., Kabaria, A., Panigrahi, B., Sammons, K., and Wilson, L., "Dynamic Weakening of CH_4-, C_2H_6-, and C_2H_4/N_2–Air Counterflow Diffusion Flames using Acoustically Perturbed Inflows." Work-in-Progress Poster Paper 4F504, Presented at 30th International Symposium on Combustion, Abstracts of Work-In-Progress Posters, The Combustion Institute, Pittsburgh, PA, July 25-30, 2004.

28. Pellett, G.L., Kabaria, A., Panigrahi, B., Sammons, K., Convery, J., and Wilson, L.G., "Dynamic Weakening (Extinction) of Simple Hydrocarbon–Air Counterflow Diffusion Flames by Oscillatory Inflows." AIAA Paper 2005-4332, July 2005, 22pp.

29. Pellett, G.L, McNamara, C., Johnson, R., Kabaria, A., Panigrahi, B., Sammons, K., Galgano, J., and Wilson, L.G., "Dynamic Weakening of Gaseous Hydrocarbon (C1-C4)–Air Counterflow Diffusion Flames by Oscillatory Inflows," to be presented at 31st International Symposium on Combustion, Abstracts of Work-In-Progress Poster Presentations, Poster 4B01, The Combustion Institute, Pittsburgh, PA, Aug. 6-11, 2006.

30. Guthhel, E., and Williams, F., 23rd *Symposium (International) on Combustion*, The Combustion Institute, Pittsburgh, 1990, p. 513.

31. Guthhel, E., Balakrishnan, G., and Williams, F., in *Reduced Kinetic Mechanisms for Application in Combustion Systems*, Lecture Notes in Physics (N. Peters and B. Rogg, eds.) Springer-Verlag, New York, 1992, p. 177.

32. Pellett, G.L., Isaac, K.M., and Nguyen, G., "Effect of Input Temperature on Strain-Induced Extinction of 50 to 100% Hydrogen–Air Counterflow Diffusion Flames," Presented at 27th Symposium (International) on Combustion, Abstracts of Work-In-Progress Poster Presentations, The Combustion Institute, Pittsburgh, PA, Poster W2D01, Aug., 1998, p. 192.

33. Rolon, J.C., Veynante, D., Martin, J.P., and Durst, E., "Counter Jet Stagnation Flows," Experiments in Fluids, **11**, (1991), pp. 313-324.

34. Spalding, D.B., "Theory of Mixing and Chemical Reaction in the Opposed-Jet Diffusion Flame," *J. Amer. Rocket Soc.*, **3** (1961), pp. 763-771.

35. Williams, F.A., "A Review of Flame Extinction," *Fire Safety J*., **3** (1981), pp. 163-175.

36. Seiser, R., Truett, L., Trees, D., and Seshadri, K., "Structure and Extinction of Non-premixed *n*-Heptane Flames," 27th Symposium (International) on Combustion, The Combustion Institute (1998), pp. 649-657.

37. Bosschaart, K.J., and de Goey, L.P.H., "The Laminar Burning Velocity of Flames Propagating in Mixtures of Hydrocarbons and Air Measured with the Heat Flux Method," *Combustion and Flame*, **136** (2004) pp. 261-269.

38. Hassan, M.I., Aung, K.T., Kwon, O.C., and Faeth, G.M., "Properties of Laminar Premixed Hydrocarbon / Air Flames at Various Pressures," *J. Propulsion and Power*, **14**, No. 4 (1998), pp. 479-488.

20-cm Speaker-driver

Fuel input

Window

Mirror on adj.mount

1.39 ∝m Laser diode (5 khz sweep)

Pyrex sleeve

N_2 purge

Porous plate

Fuel

Ceramic insulation jacket

Pyrex

Flame

Pyrex

Air

Pyrex window

Ceramic paper enclosure

Argon bath gas

Focusing Schlieren System used here to visualize flows and disk-shaped flame structure, in horizontal direction. (Details in Pellett et al., AIAA-94-2300, and also AIAA-95-3112)

N_2 purge

Mirror on adj.mount

CCD detector

Window

Oxidizer input

GP07262K

Fig. 1a. Schematic of Oscillatory Opposed Jet Burner (OOJB) system with twin 20-cm speaker-drivers. Diode laser system is passive in this study.

13
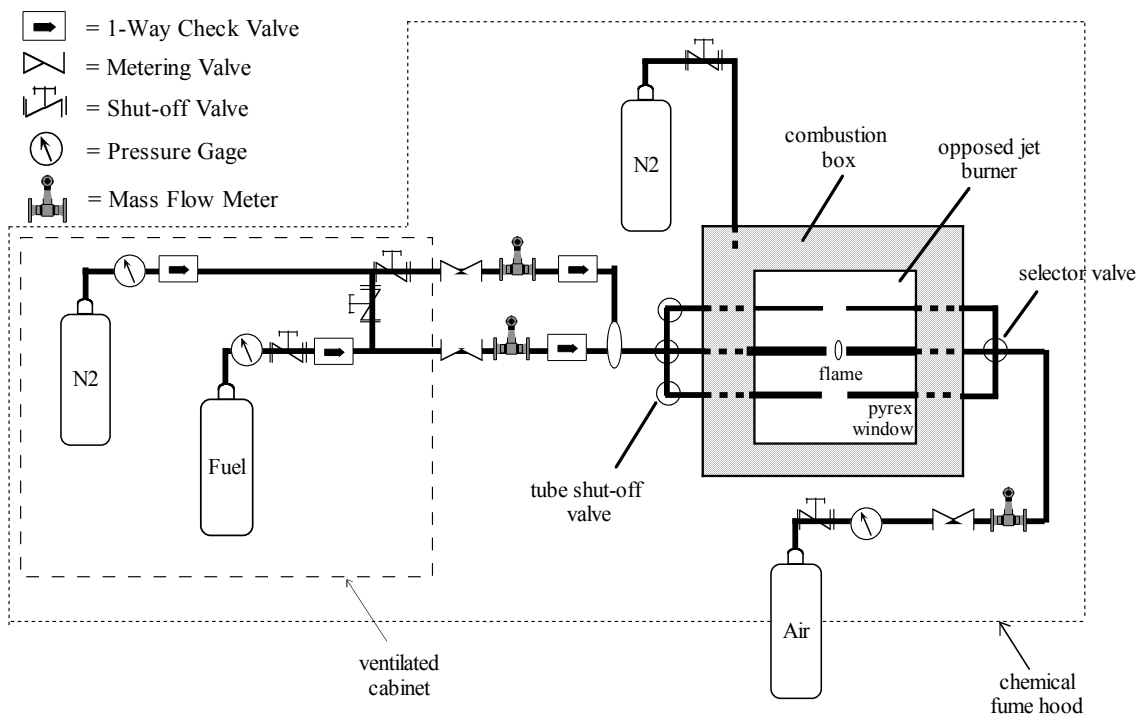
Fig. 1b. Gaseous-Fuel Horizontal-Tube Opposed Jet Burner (OJB) test schematic (not to scale). Combustion box, constructed of 0.5 in thick compacted silica fiber-board panels, has a porous metal plate on top -- typically 4 x 6 in is exposed and "active". Thus combustion products are actively purged by controlled nitrogen flows from two porous plug outlets at opposite corners of the box floor. The three matching sets of tube-OJBs are actually arrayed in a horizontal plane, not vertically as shown. Mass flows of fuel, fuel-diluent, and air are monitored more or less continuously as flame extinction and restoration limits are approached and achieved.
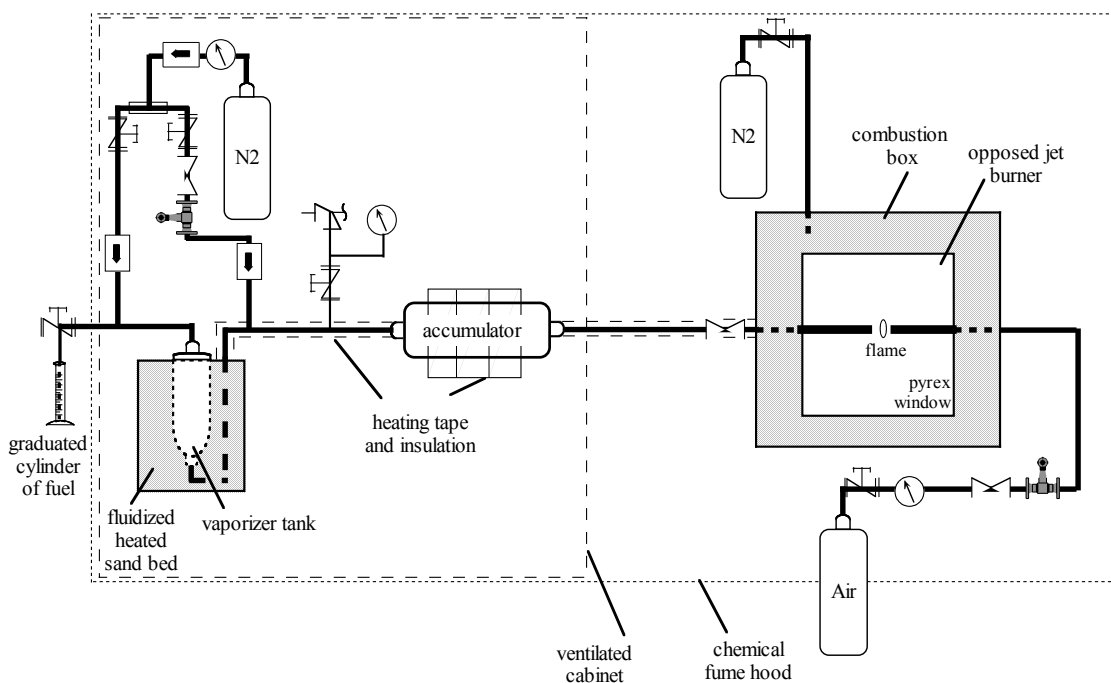
Fig. 1c. Liquid Fuel Opposed Jet Burner test schematic (not to scale). Silica fiber combustion box, with porous plate on top, is identical to that in Fig. 1b. Vaporizer tank is 0.5 L and accumulator tank is 9.5 L. For each batch test (set), a known volume of liquid HC is injected into the cold, evacuated system. Then mass-flow-metered fuel diluent (either N_2 or gaseous HC) is admitted, up to a specific pressure. Finally, the system is sealed and heated to a measured (multipoint averaged) temperature and pressure, and held there to assure mixing, before it is operated in a "blow down mode" to supply the 7.5 mm tube-OJB system. For the vaporized liquid HC experiments, air mass flows are monitored, but the mass flows of fuel mixture are generally not monitored due to temperature limitations.
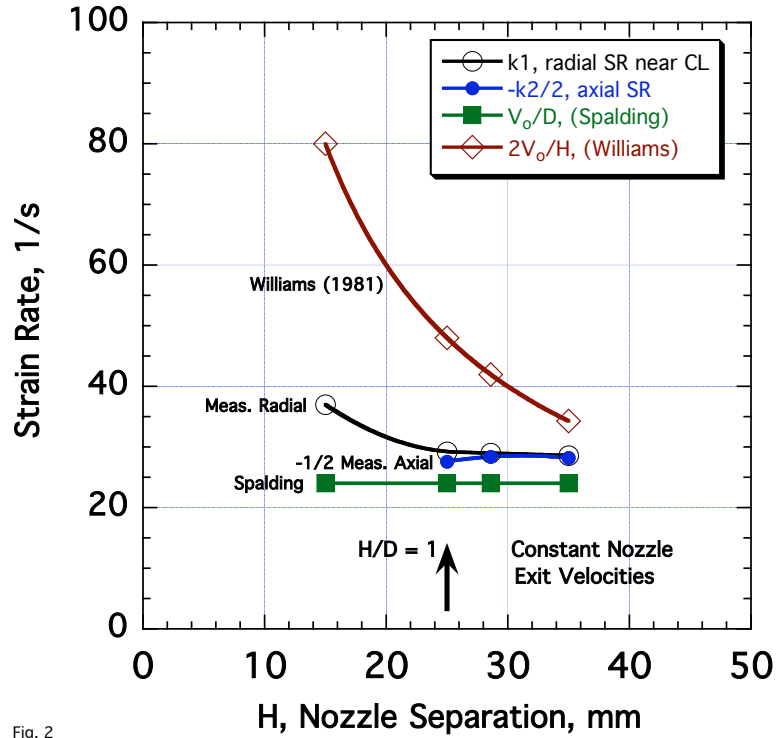
Fig. 2

Fig. 2. Comparison of Rolon's LDA-Measured Strain Rates
for Variable Separation of 25 mm Contoured Nozzles, Air
vs Air. Rolon et. al, Exp. in Fluids, **11** (1991) pp. 313-324.
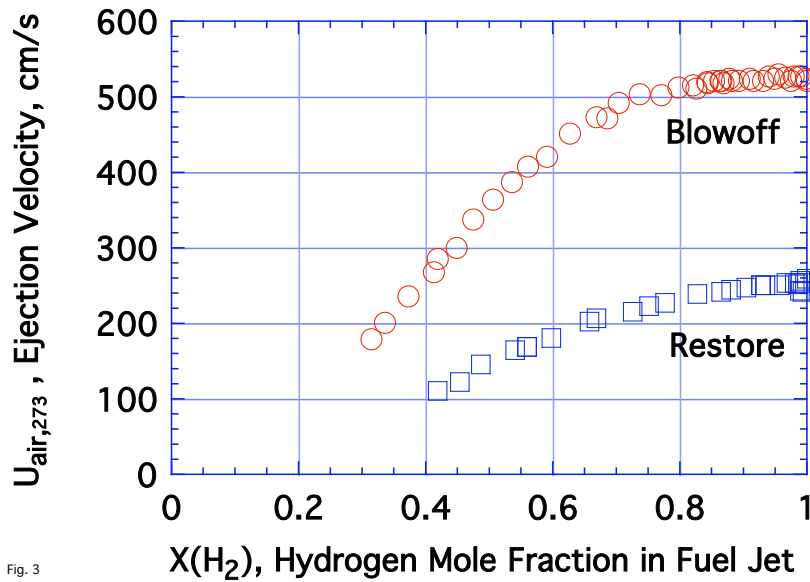
Fig. 3

Fig. 3. Air Flows, Extinction and Restoration of N_2-diluted H_2 vs Air
CFDFs, using 2.7 mm Horizontal-Tube-Opposed Jet Burner.
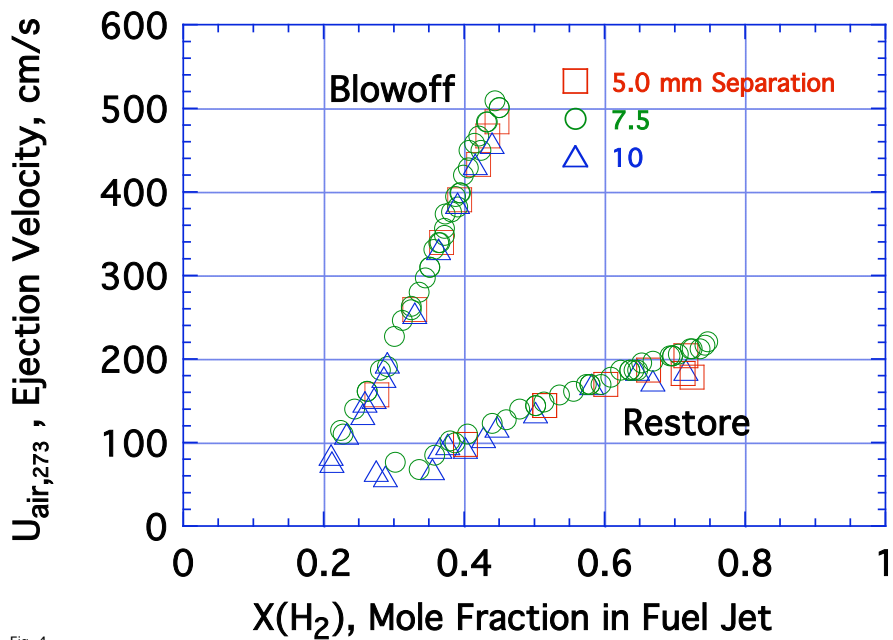
Fig. 4

Fig. 4. Effect of Tube Separation on Extinction and Restoration of H_2/N_2—Air CFDFs, using 5.0 mm Horizontal-Tube-OJB.
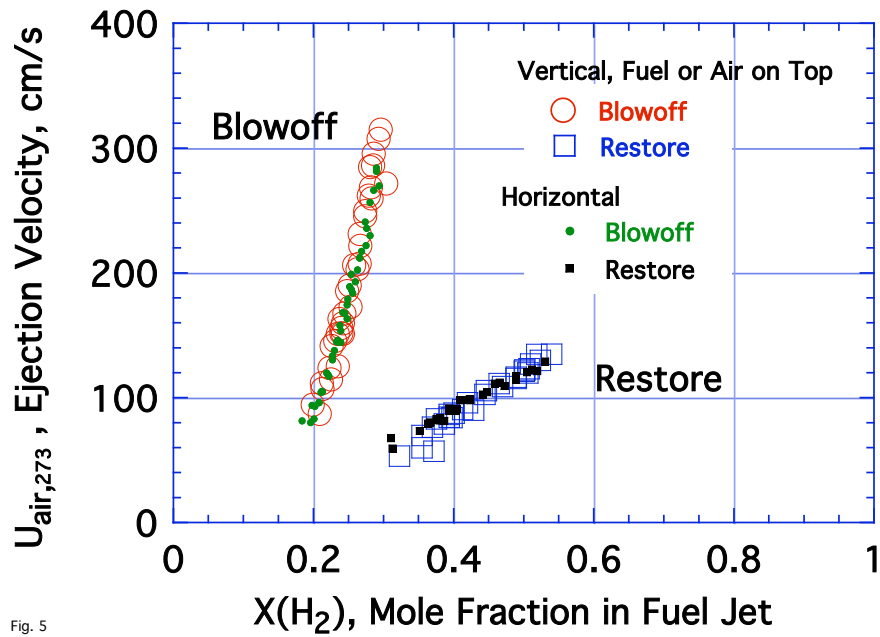
Fig. 5

Fig. 5. Effect of Orientation on Extinction & Restoration of H_2/N_2—Air CFDFs, using Vertical & Horizontal 7.0 mm Pyrex Tube-OJBs.
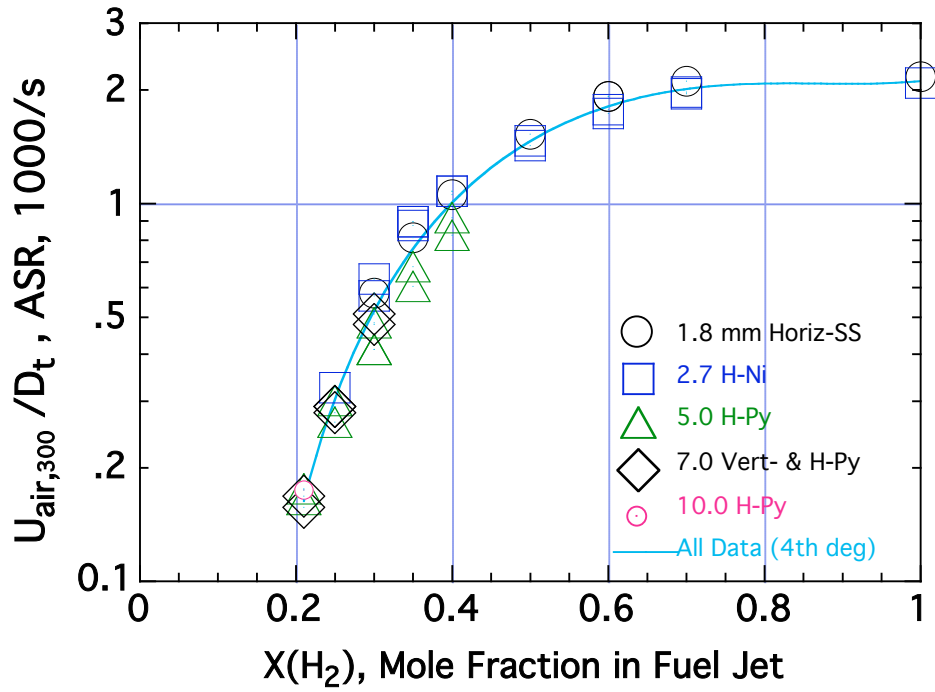
ig. 6

Fig. 6. Applied Stress Rates (ASR) for Tube-OJBs, at 300 K
Airside Edge of Flame, for Extinction of H_2/N_2—Air CFDFs.
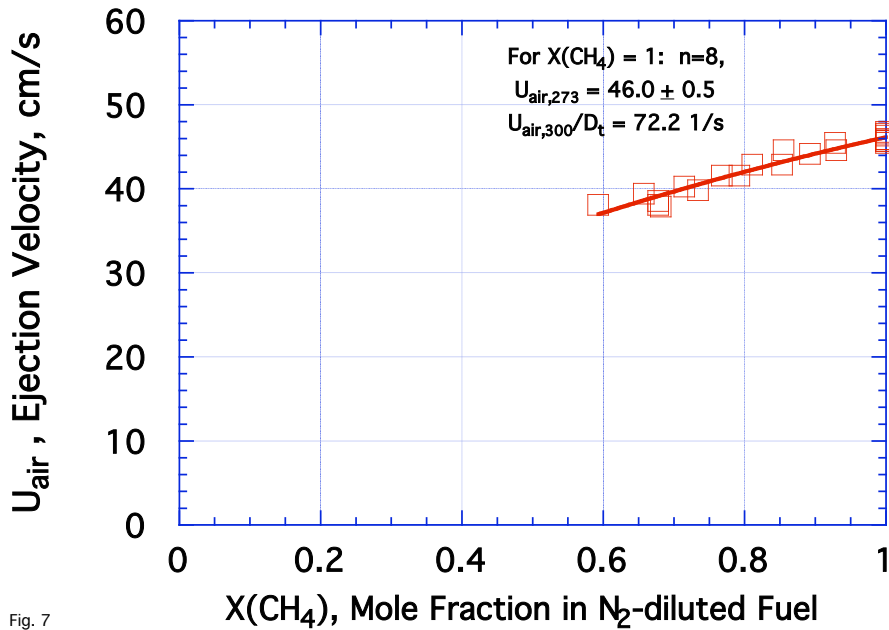
Fig. 7

Fig. 7. Extinction of CH_4/N_2—Air CFDFs, using 7.0 mm Vertical-
Tube-OJB (fuel on top).
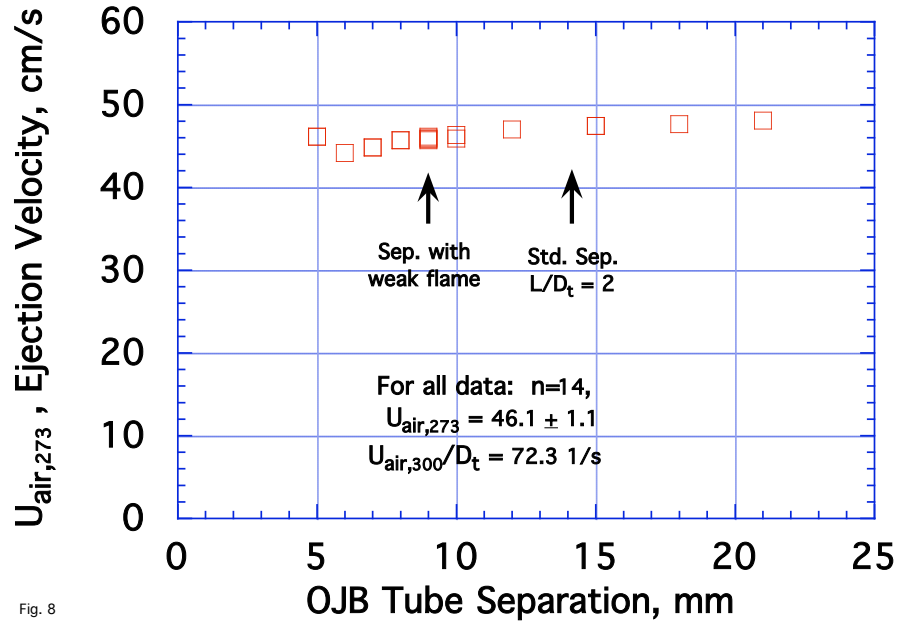
Fig. 8

Fig. 8. Effect of Tube Separation on Extinction of CH_4 vs. Air CFDFs, using 7.0 mm Horizontal-Tube-OJB.
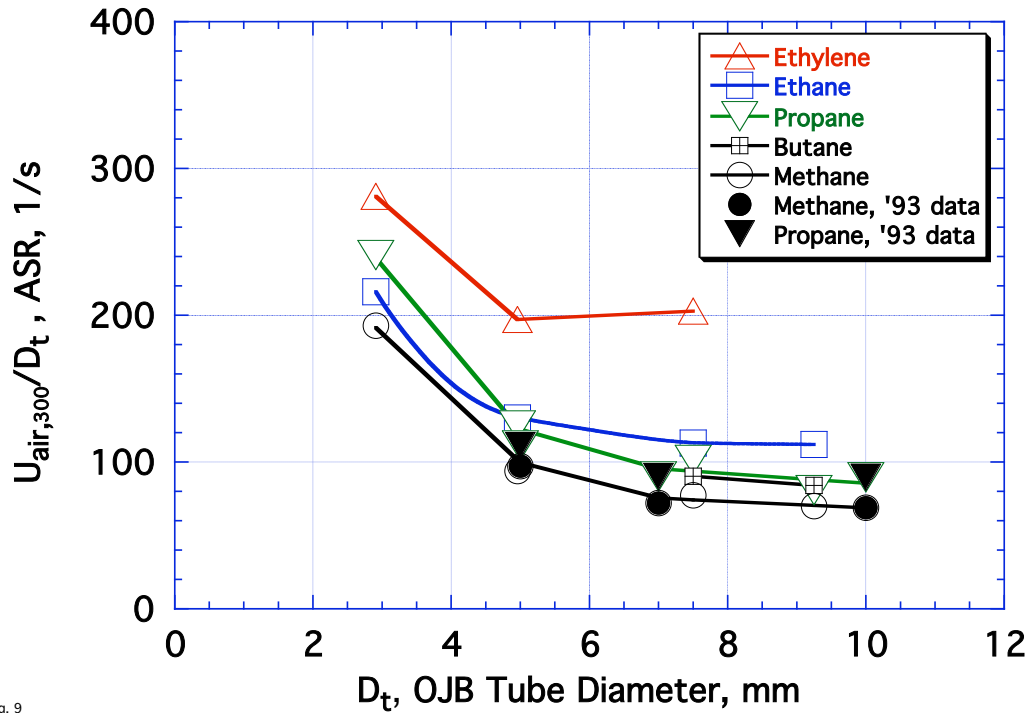
Fig. 9

Fig. 9. Effect of OJB Tube Diameter on Applied Stress Rate at Extinction, for Various Gaseous Hydrocarbon vs Air CFDFs.

18
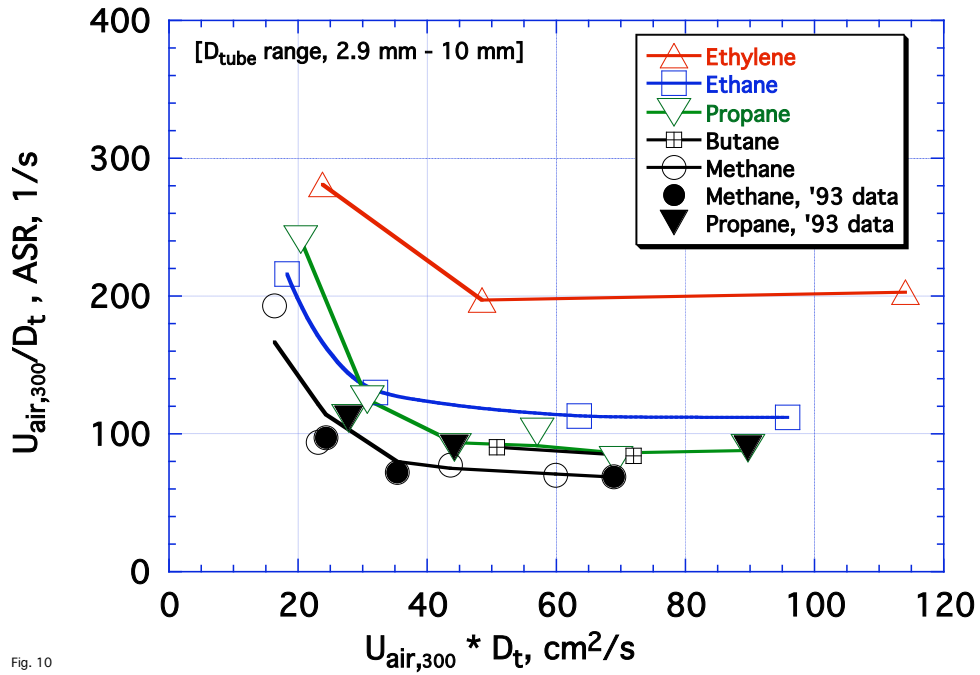
Fig. 10. Asymptotic Approach of Applied Stress Rates (ASRs) at Extinction, as Functions of Exit-Velocity * Tube-Diameter Product (~ *Re*) for Various Gaseous HC vs Air CFDFs.
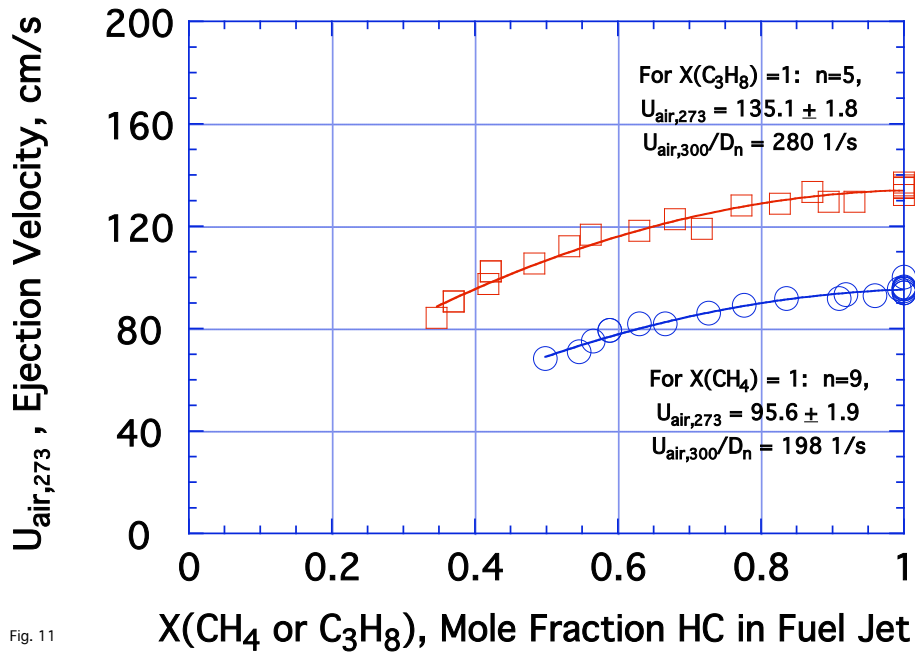
Fig. 11. Extinction of CH_4/N_2—Air and C_3H_8/N_2—Air CFDFs, using 5.3 mm Brass Horizontal-Nozzle OJB.
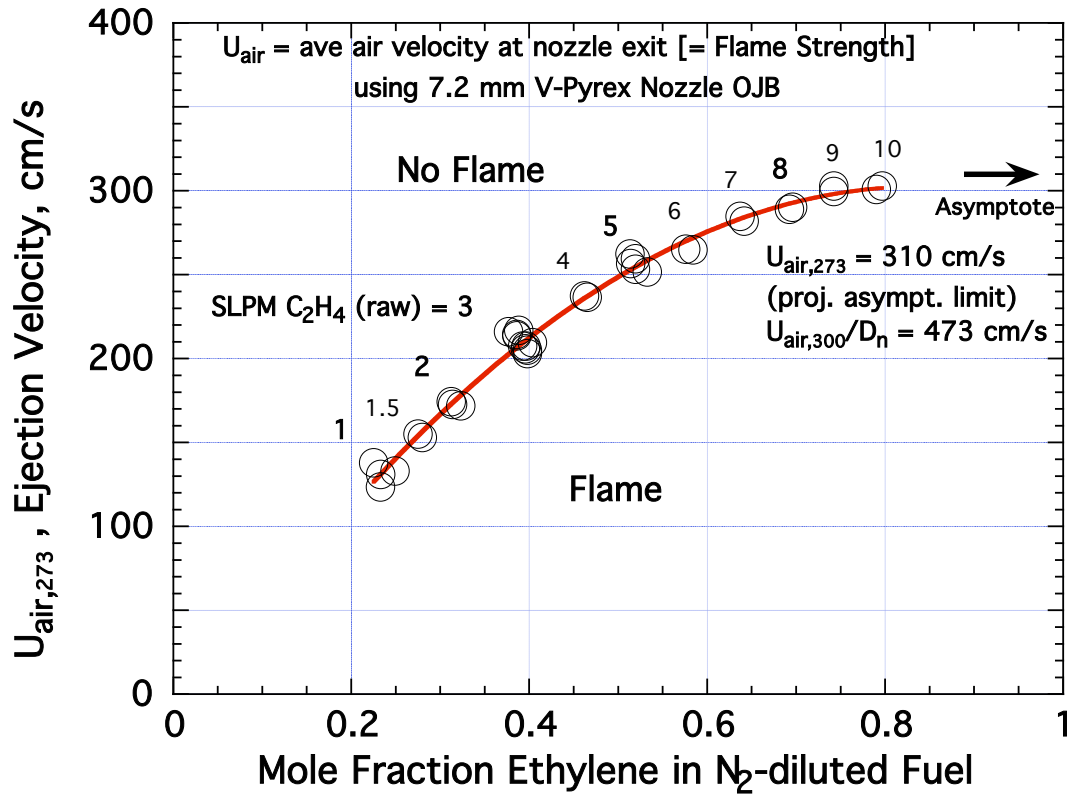
Fig. 12. Steady-State Extinction of C_2H_4/N_2—Air Counterflow Diffusion Flames, using 7.2 mm Vertical-Pyrex Nozzle OOJB.
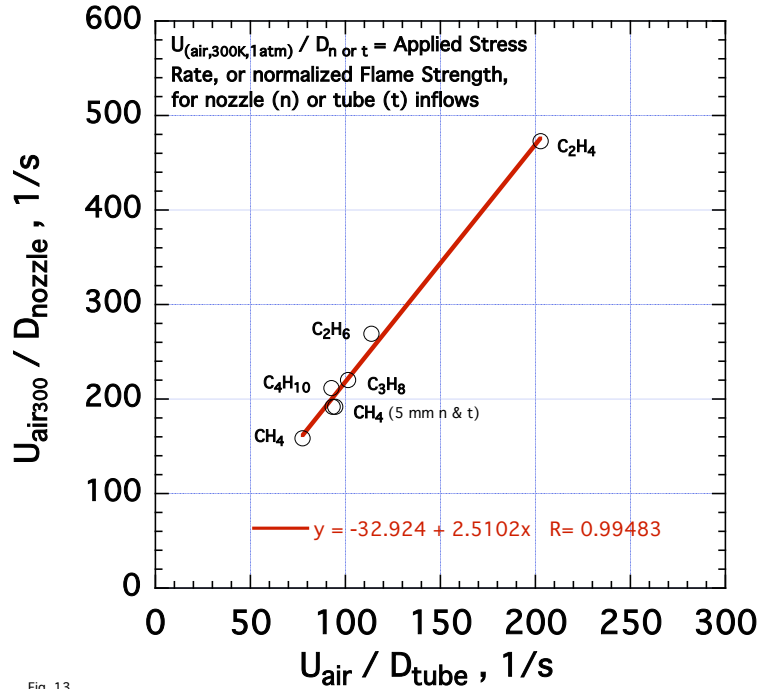
Fig. 13. OJB-Extinction-Limit "Idealized Flameholding Scale," from 7.2 mm Convergent Nozzle- and 7.5 mm Straight Tube-OJBs, for Methane, Propane, Butane, Ethane, and Ethylene–Air CFDFs.
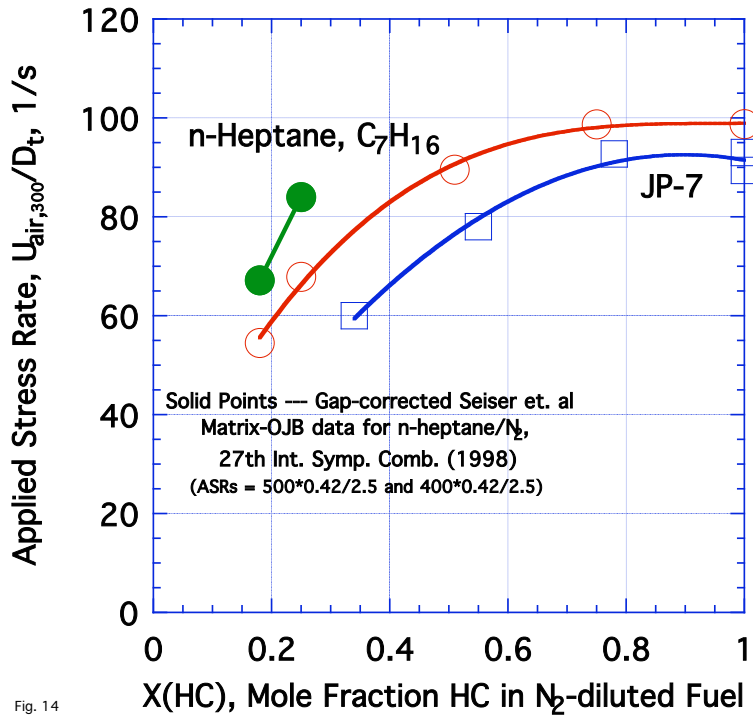
Fig. 14. Extinction of *n*-Heptane/N_2–Air and JP-7/N_2–Air CFDF's, using 7.5 mm Tube-OJB with Batch Vaporizer System; and comparison with Gap-Corrected Seiser et. al Heptane Data [36].
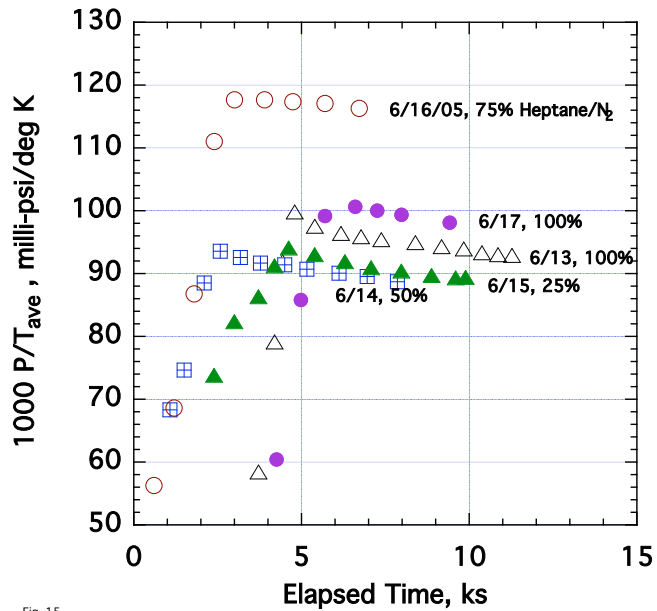
Fig. 15

Fig. 15. Rise & Decay of Pressure / Temperature Ratio (~moles fuel), for n-Heptane Vaporization in N_2, followed by a small leak (in a valve).
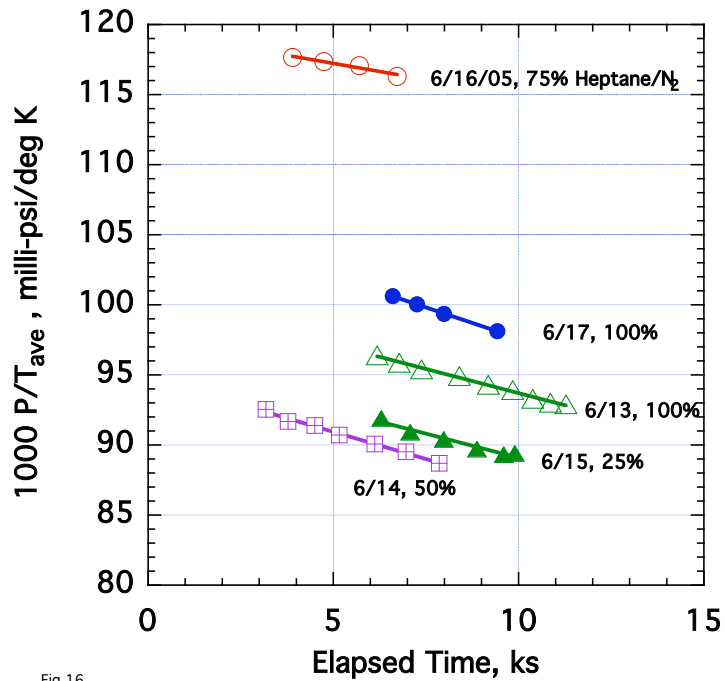
Fig 16

Fig. 16. Decay of Pressure / Temperature Ratio (~ moles fuel), for n-Heptane Vaporization in N_2, followed by a small leak (in a valve).

22
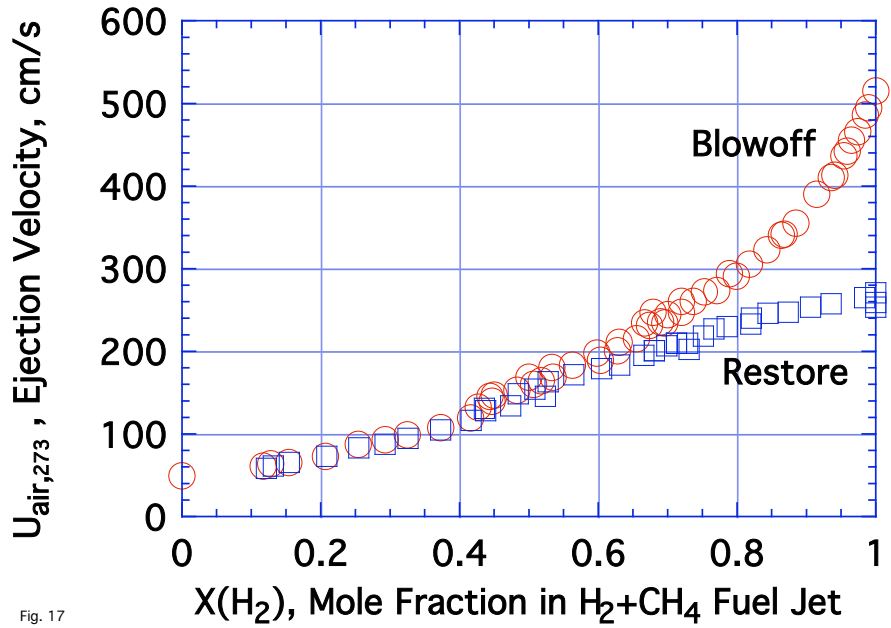
Fig. 17. Effect of Methane Reactivity (w/H-atom) on Extinction and Restoration of CH_4-diluted H_2 vs Air CFDFs, using 2.7 mm Tube-OJB.
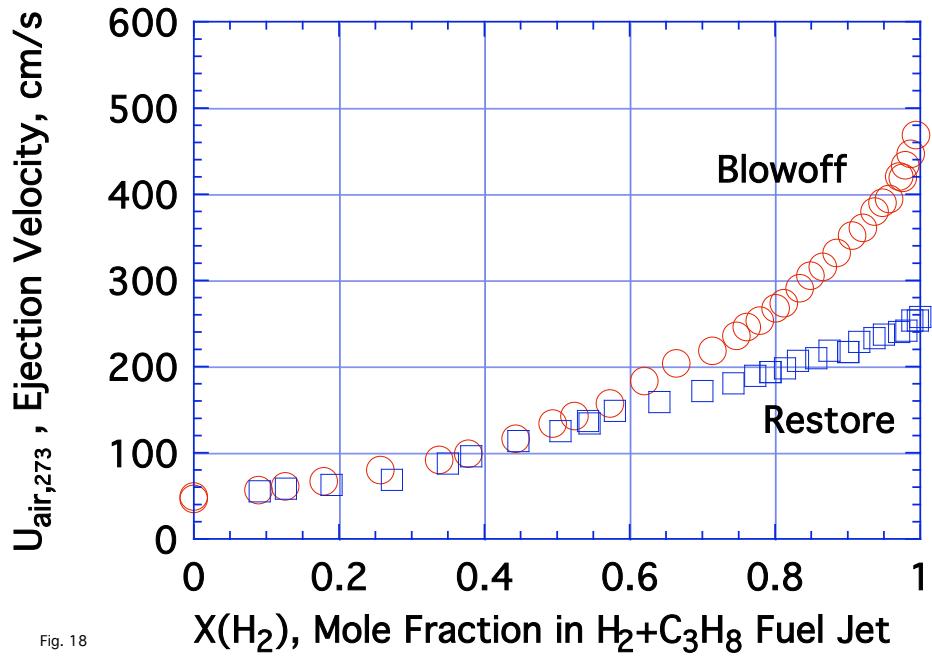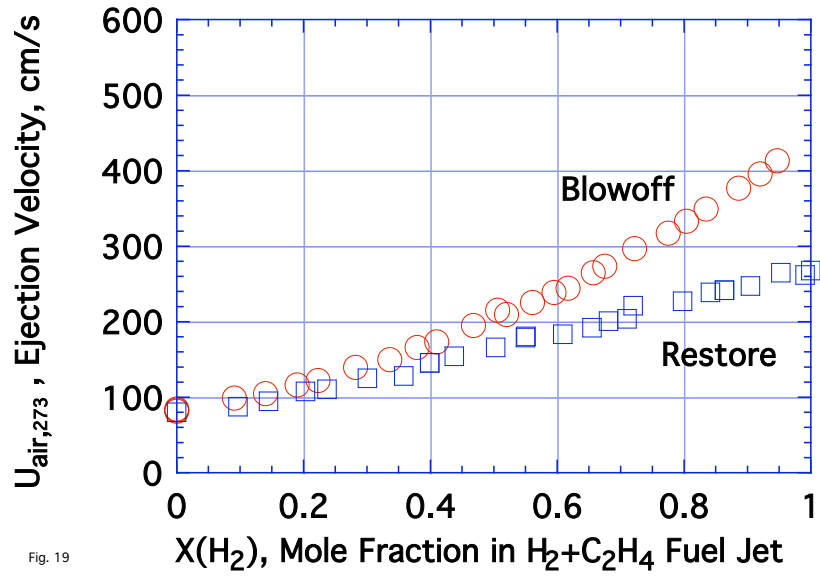

Fig. 18. Effect of Propane Reactivity (w/H-atom) on Extinction and Restoration of C_3H_8-diluted H_2 vs Air CFDFs, using 2.7 mm Tube-OJB.

Fig. 19

Fig. 19. Effect of Ethylene Reactivity (w/H-atom) on Extinction and Restoration of C_2H_4-diluted H_2 vs Air CFDFs, using 2.7 mm Tube-OJB.
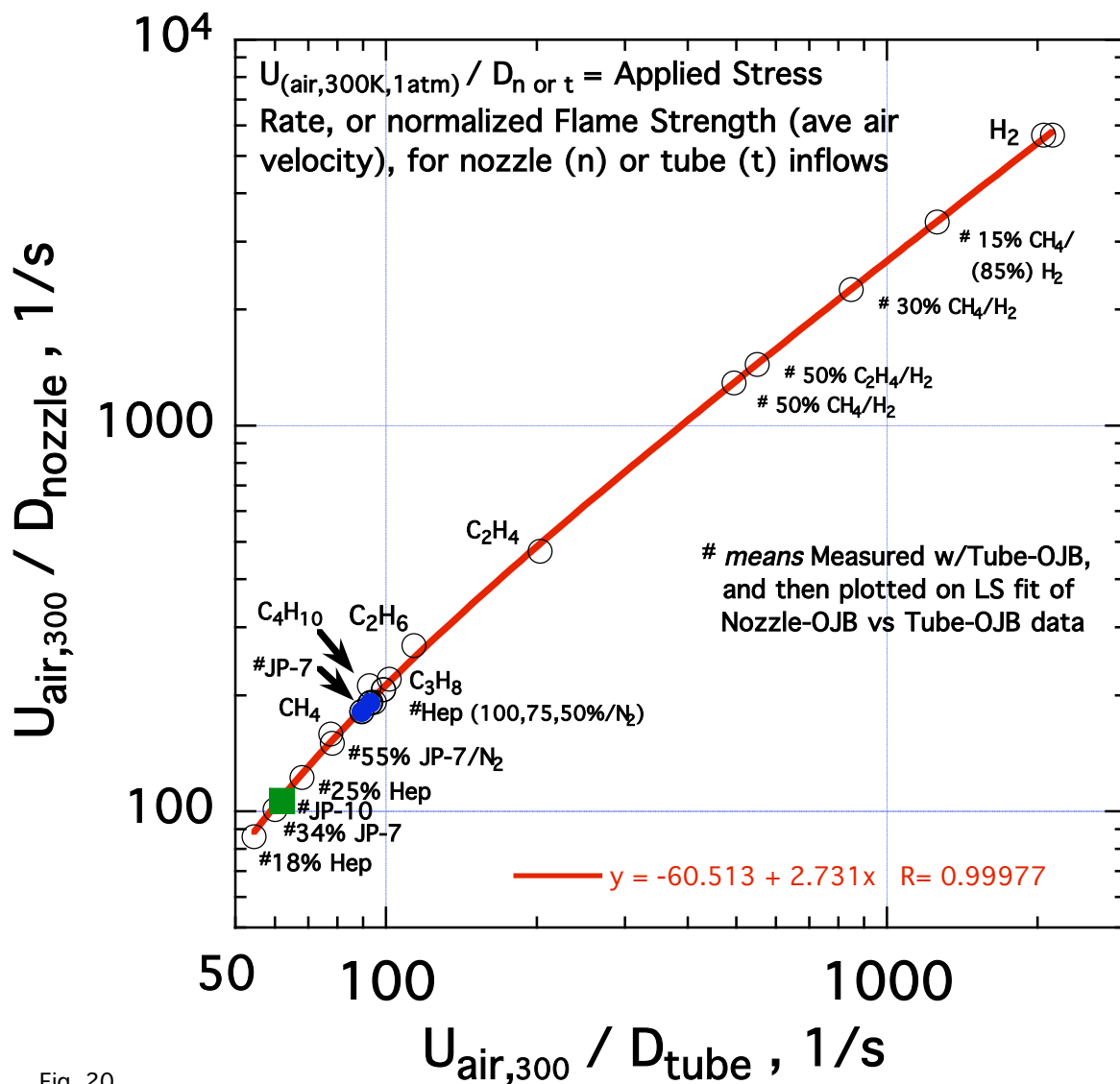
Fig. 20

Fig. 20. OJB-Extinction-Limit "Idealized Flameholding Scale" from Convergent-Nozzle- and Straight-Tube-OJBs, for JP-7, JP-10 and *n*-Heptane / Nitrogen; and Methane, Propane, Butane, Ethane, Ethylene, and Hydrogen–Air CFDFs.
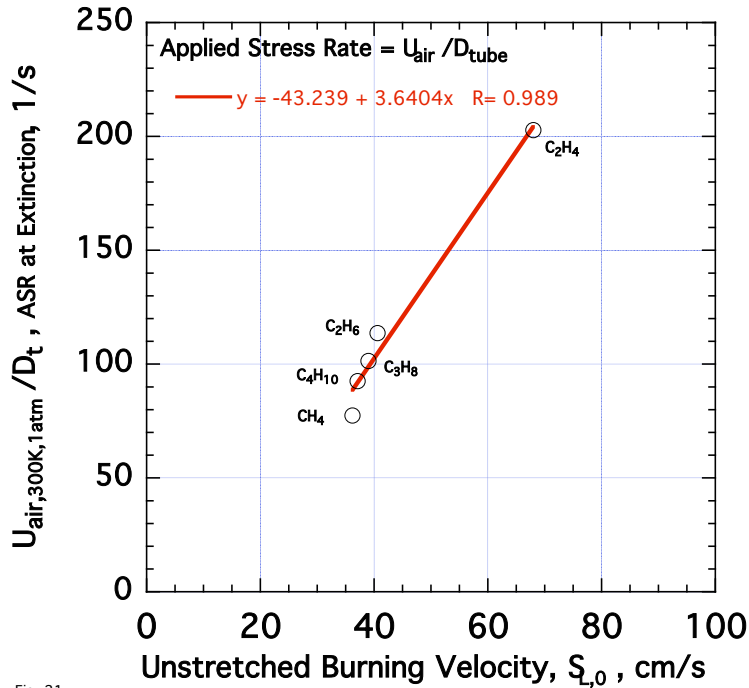
Fig. 21

Fig. 21. Comparison of Extinction Limits, from 7.5 mm Tube-OJB, with Unstretched Laminar Burning Velocity at phi = 1, for Methane, Ethane, Propane, Butane and Ethylene–Air Flames.
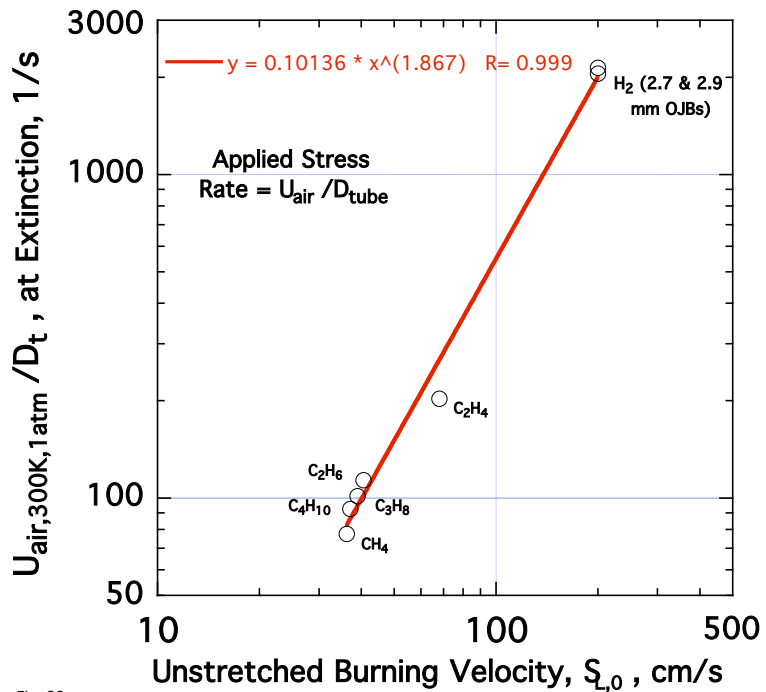

Fig. 22

Fig. 22. Comparison of Extinction Limits, from 7.5 mm Tube-OJB, with Unstretched Laminar Burning Velocity at phi = 1, for Methane, Ethane, Propane, Butane, Ethylene **and** H_2–Air Flames.

26